2021

# A Numerical Study on the Pool Boiling with Foam Surface Enhancement Using Different Refrigerants

Mingkan Zhang
*Oak Ridge National Laboratory, United States of America*, zhangm1@ornl.gov

Kashif Nawaz

Cheng-Min Yang

Matthew Sandlin

William Asher

*See next page for additional authors*

# A Numerical Analysis of The Pool Boiling Process in Flooded Evaporators Using Different Refrigerants

Mingkan Zhang[1], Kashif Nawaz[1]*, Cheng-Min Yang[1], Matthew Sandlin[1], William Asher[1], Brian Fricke[1], Anthony C. Gehl[1],

[1]Oak Ridge National Laboratory, Energy Science and Technology Directorate,
Oak Ridge, TN, USA

* Corresponding Author

## ABSTRACT

The pool boiling process can be observed in several energy conversion processes including commercial and industrial refrigeration, industrial air-cooling operations, and power generation. The process becomes more involved when pool boiling in a tube bundle is considered. In the current study, a numerical model is developed to predict the key performance parameters of a flooded evaporator while considering a range of working fluids. A kettle reboiler configuration was considered, and a performance model was developed to account for boiling on individual tubes, merging of vapor bubbles, and movement under gravity. A volume of fluid (VOF) model was used to deal with the different phases in the simulation. Various fluids were considered in this study including HFE-7000, HFE-7300, and water. The trajectories of the bubbles were tracked, and the resulting information has been summarized in physical measurable quantities.

## 1. INTRODUCTION

Kettle reboilers are commonly used as shell and tube heat exchangers with a tube bundle placed in the shell. In the reboiler, the fluid boils on the outside of the tubes when it is heated by the tube bundle. A natural convection is induced by the density difference between the two-phase mixture flowing. The mixing flow in the tube bundle and between the tube bundle and the shell wall leads to a natural circulation in the reboiler. Such reboilers are widely used in the process industry, so it is desired to develop a model to predict the boiling process in the kettle reboiler. Therefore, lots of efforts have been dedicated to build kettle reboiler models.

The one-dimensional model is the simplest approach, in which two main assumptions were employed. First, it assumes that liquid enters each column of the tube bundle from the bottom and evaporates as it moves vertically upwards (Brisbane et al., 1980; Jensen, 1988). The second assumption is that the two-phase pressure drop in a column is assumed to balance with the liquid static head. Void fraction and two-phase friction multiplier correlations are required to complete the model in order to include the effects of natural convection and friction. Therefore, the key of the one-dimensional model is to seek the two correlations from empirical data. Although some studies provide void fraction and two-phase friction multiplier correlations, best agreement with the available experimental data, Burnside et al. (Burnside et al., 2001) has concluded that the one-dimensional model is only valid at heat fluxes lower than 20 $kW/m^2$ due to its inherent assumptions.

Two-dimensional models were developed due to the limitations of the one-dimensional model. Because of the complexity of the boiling process in the kettle reboiler, one attempt at two-dimensional flow is using one fluid to describe the motion of the two-phase mixture flowing by assuming that the two phases move in the same direction with different velocities per phase. As a result, the one-fluid, two-dimensional model also requires two correlations to make it complete. Some applications of the two-dimensional model have been reported (Burnside, 1999; McNeil, Bamardouf, & Burnside, 2010). However, such two-dimensional models still cannot break through the 20 $kW/m^2$ limitation since it has been reported that the predicted pressure distributions using the one-fluid two-dimensional

model did not agree with the measured values of Burnside et al. (Burnside et al., 2001) and McNeil et al. (McNeil, Bamardouf, Burnside, et al., 2010), where significant deviations from the static liquid pressure distributions were reported for heat fluxes greater than 20 kW/m$^2$.

On the other hand, the two-dimensional model of kettle reboilers considering two fluids has also been developed (Edwards & Jensen, 1991). Since the two fluids model is able to calculate void fraction using the fractions of both fluids, the correlation for void fraction is no longer required. As a result, only the correlation for the drag coefficient is needed for this model. Different approaches have been reported to obtain the correlation, including from data taken for vertical two-phase flow across a horizontal tube bundle (Rahman et al., 1996), from the air–water data of (R Dowlati et al., 1992; Ramin Dowlati et al., 1990; Schrage et al., 1988) as a power law function of the Reynolds number, and from air–water measurements (Pezo et al., 2006; Stevanovic et al., 2002; Stosic & Stevanovic, 2002). In the last approach, two correlations for the drag coefficient were proposed: one for the bubbly flow regime and another for the churn flow regime. Although the reported two-dimensional models of the reboiler can capture some features of boiling process, more and more introduced correlations in such models made them too reliant on experimental corrections. As a result, those models are not easy to implement since they might only apply to very specific cases wherein the correlations work.

The goal of the present research is to both develop a two-dimensional direct CFD model to describe the flow and heat transfer in a kettle reboiler without introducing any correlations as well as a preliminary study of modeling flow and heat transfer in a flooded evaporator with changeable surface structures. A volume of fluid (VOF) model was used to handle the different phases in the simulation. Multiple fluids were tested in the pool boiling process, including HFE-7000, HFE-7300, and water. HFE-7000 and HFE-7300 were selected ecause boiling points of HFE-7000 and HFE-7300 are close to room temperature (34 °C) and water's boiling point (98°C), respectively.

## 2. NUMERICAL METHOD

A 2D model has been developed to simulate the heat transfer process. Based on the mass and momentum balances, the continuity and momentum equations are introduced to describe the motion of the fluids in the flooded evaporator. In the present model, the liquid and vapor phases of the fluids are considered, with evaporation occurring in the flooded evaporator. Therefore, a volume of fluid (VOF) model is employed to describe the multiple phase flow and heat transfer, as well as the evaporating process. In the VOF model the continuity equation can be written as

$$\frac{\partial \rho_m}{\partial t} + \nabla \cdot (\rho_m \vec{v}_m) = 0, \tag{1}$$

where $\vec{v}_m$ is the mass averaged velocity and $\rho_m$ is the mixture density, as

$$\vec{v}_m = \frac{\sum_{i=1}^{n} \alpha_i \rho_i \vec{v}_i}{\rho_m} \tag{2}$$

and

$$\rho_m = \sum_{i=1}^{n} \alpha_i \rho_i \tag{3}$$

with $\alpha_i$ as the volume fraction of phase *i*. *n* is the number of phases. In the present work *n* = 2, while *i* = 1 and 2 represent liquid and vapor, respectively.

The equation for the liquid volume fraction $\alpha_1$ is,

$$\frac{\partial (\rho_1 \alpha_1)}{\partial t} + \nabla \cdot (\rho_1 \alpha_1 \vec{v}_1) = (\dot{m}_{21} - \dot{m}_{12}), \tag{4}$$

where $\dot{m}_{21}$ and $\dot{m}_{12}$ are the mass transfer from vapor to liquid, and from liquid to vapor, respectively. Vapor volume fraction is calculated by $\alpha_1 + \alpha_2 = 1$.

The VOF model (Hirt & Nichols, 1981; Noh & Woodward, 1976) form of the momentum equation is

$$\frac{\partial (\rho_m \vec{v}_m)}{\partial t} + \nabla \cdot (\rho_m \vec{v}_m \vec{v}_m) = -\nabla p + \nabla \cdot [\mu_m (\nabla \vec{v}_m + \nabla \vec{v}_m^T)] + \rho_m \vec{g} + \nabla \cdot \left(\sum_{k=1}^{n} \alpha_i \rho_i \vec{v}_{dr,i} \vec{v}_{dr,i}\right), \tag{5}$$

where $p$ is the pressure,

$$\mu_m = \sum_{i=1}^{n} \alpha_i \mu_i, \tag{6}$$

is the viscosity of the mixture and $\vec{v}_{dr,i}$ is the drift velocity for phase *i*,

$$\vec{v}_{dr,i} = \vec{v}_i - \vec{v}_m. \tag{7}$$

The Energy Equation is

$$\frac{\partial}{\partial t} \sum_{i=1}^{n} (\alpha_i \rho_i E_i) + \nabla \cdot \sum_{i=1}^{n} (\alpha_i \vec{v}_i (\rho_i E_i + p)) = \nabla \cdot (\lambda_{\text{eff}} \nabla T), \tag{8}$$

where $\lambda_{\text{eff}}$ is the effective conductivity and

$$E_i = h_i - \frac{p}{\rho_i} + \frac{v_i^2}{2}. \quad (9)$$

*E* is the total energy including terms of sensible enthalpy, pressure work, and kinetic energy. In the present model, real gas model is employed for air and vapor. The flows are turbulent, so a standard *k-ε* model (ANSYS, 2017) is introduced.

A commercial code ANSYS/FLUENT is employed to build the geometry model, generate the mesh, and solve the mathematic models.

## 3. MODEL VALIDATIONS

### 3.1 Single Tube Validation

The model was quantitatively validated by comparing to a single tube experiment accomplished at ORNL. In the experimental setup, a horizontal copper tube was placed in a reservoir filled with refrigerant 3M™ HFE-7300 Engineered Fluid (properties showing in Table 1). The size of reservoir is 9" by 9" with 4" height, in the center of which the single tube is located. When the heater inside of the tube heats the reservoir and HFE-7300 reaches its saturation temperature and pressure, boiling was observed. By controlling the power of the heater, the heat flux on the outside of the tube was varied. Meanwhile, the temperature on the tube surface was measured in order to calculate the excess surface temperature: $T_{excess} = T_{surface} - T_{boiling}$. Based on the experimental setup, a two-dimensional numerical model was built as shown in Figure 1. Using the model, a steady-state simulation was conducted. Figure 2 shows the volume fraction of liquid in the simulation domain. Table 2 shows a comparison of excess temperatures between experimental data and simulation results. Consequently, the comparison shows a quantitative match between experimental data and numerical results.

**Table 1:** Thermal properties of water, HFE-7000, and HFE-7300 (3M, 2009, 2014)

| | water | HFE-7000 | HFE-7300 | pentane |
|---|---|---|---|---|
| $T_{boiling}$@ 1 atm (°C) | 100 | 34 | 98 | 36 |
| Latent heat (kJ/kg) | 2442.3 | 142 | 101.7 | 367.3 |
| Liquid density ( kg/m$^3$) | 997.1 | 1400 | 1660 | 626 |
| Gas density ( kg/m$^3$) | 0.023 | 5.59 | 0.875 | 2.97 |
| Liquid specific heat (kJ/kg K) | 4.18 | 1.3 | 1.14 | 2.37 |
| Liquid thermal conductivity (W/m K) | 0.61 | 0.075 | 0.063 | 0.107 |
| Fluid viscosity( N·s/m$^2$)\| ( Pa·s) | 0.00089 | 0.00045 | 0.00118 | 0.000199 |
| surface tension (N/m) | 0.072 | 0.0124 | 0.015 | 0.014 |

**Table 2:** Comparison of excess temperature between experimental data and simulation results

| Heat flux (W/m$^2$) | Experimental excess surface T(°C) | Numerical excess surface T(°C) |
|---|---|---|
| 17682 | 5.13 | 3.77 |
| 28577 | 6.01 | 6.49 |
| 39313 | 6.78 | 10.99 |
| 50206 | 7.14 | 12.10 |

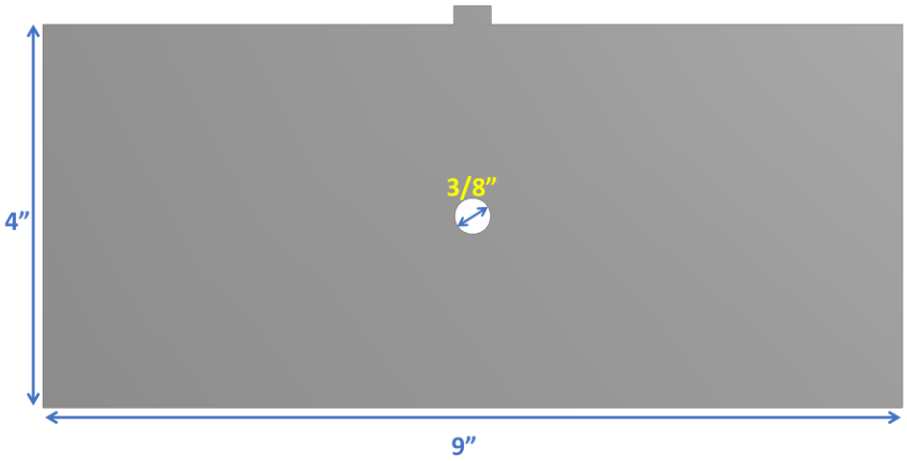


**Figure 1:** Schematic view of the single tube validation model.

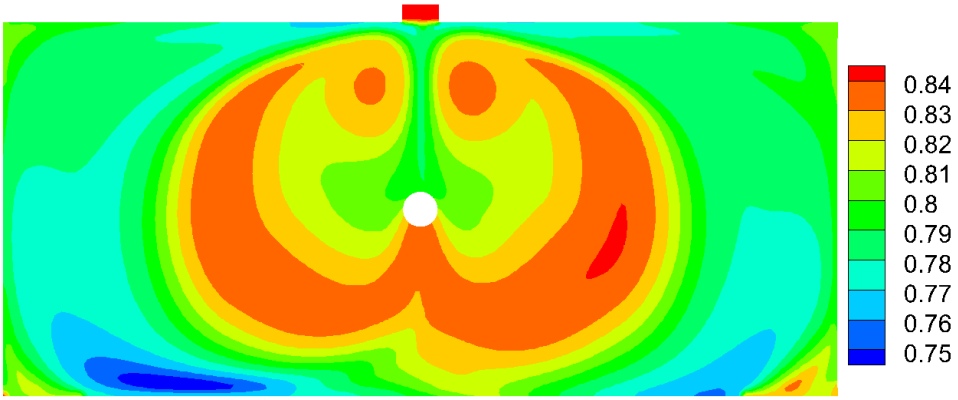


**Figure 2:** Volume fraction of liquid in the simulation domain.

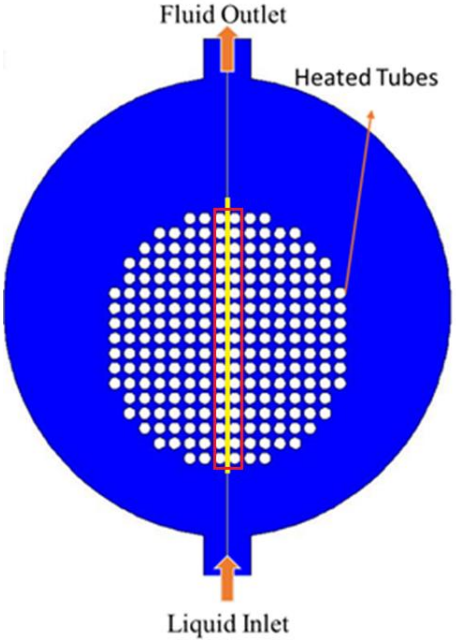


**Figure 3:** A schematic view of the simulation domain. The yellow line is the symmetric line of the reboiler crossing two ends of the tube matrix.

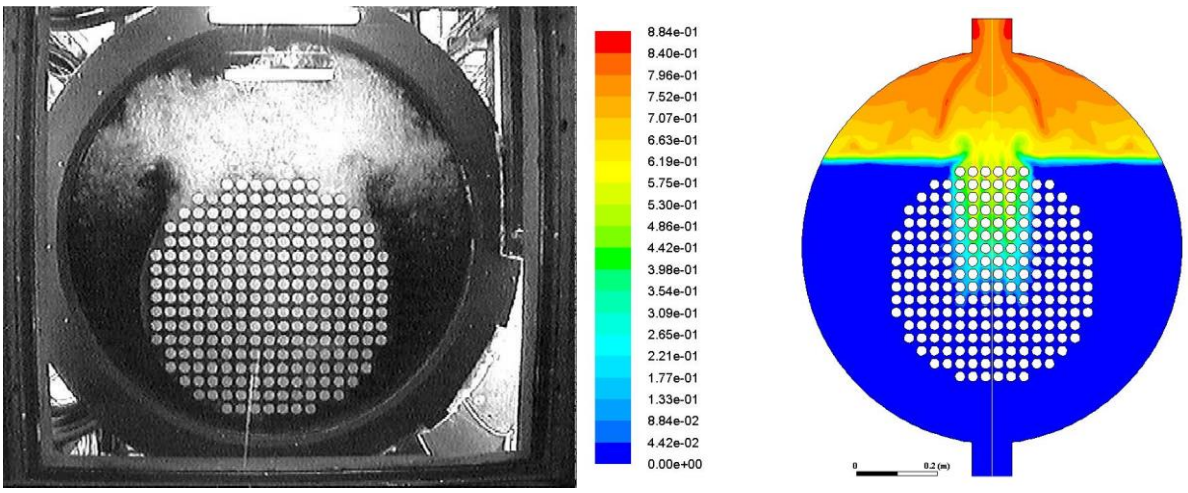


**Figure 4:** Comparison of results from McNeil et al. (McNeil, Bamardouf, Burnside, et al., 2010) and present model.

### 3.2 Kettle Reboiler Validation

In addition to the single tube validation, a further validation was conducted by comparing numerical results and experimental data about boiling in a kettle reboiler. To efficiently use computational resources, a symmetric model was built to capitalize on the symmetry of the reboiler.

The size of the reboiler is based on a real device reported by McNeil et al. (McNeil, Bamardouf, Burnside, et al., 2010). The shell is 230 mm in diameter and contains, a matrix of 224 tubes with a diameter of 19 mm. The distance between adjacent tubes is 5 mm edge to edge. After the liquid is injected from the bottom of the reboiler, it is heated by the tubes, changes phase from liquid to vapor, and then leaves the reboiler through the outlet at the top of the reboiler.

To validate the model, an experiment in the literature has been duplicated by using present model. Note that in the validation, the boiling liquid is pentane to be consistent with the literature, and the properties of which are from NIST (Lemmon; et al., 2020). Figure 4 shows the comparison of the liquid/vapor distribution in a profile of the reboiler between experiment and simulation results. It shows the patterns of vapor distribution are very close to each other and a good agreement between experimental data and simulation exists. The simulation result also shows that above certain height of the tube matrix, boiling happens within a rectangular area. It is because when the water is flowing upwards through the matrix, it absorbs heat from the tubes. After the water is above the certain height of the tube matrix, it has absorbed enough heat to start boiling. On the other hand, only in the center of the tube matrix, heat of water can accumulate to reach the boiling point. Therefore, the combined factors make the boiling happening within a rectangular area in the tube matrix above certain height.

## 4. RESULTS AND DISCUSSIONS

The model was implemented to study the boiling phenomena for water, HFE-7000 and HFE-7300 in a reboiler. In the simulations, two fluxes were applied to the tubes, 30 KW/m$^2$ and 50 KW/m$^2$. After a certain time (typically 60 s), the boiling will be fully developed and the vapor volume fraction fixed, indicating steady-state conditions have been reached. All of the following results in this section are the result of when the reboiler has reached steady state, when the fractions of each phase are in steady state, and liquid/vapor distribution pattern does not change. To investigate the boiling process for different refrigerants, data were collected near the tube matrix along the symmetric line of the reboiler as shown in Figure 3 (yellow line). The two ends of the yellow line indicate the refrigerants at the entrance and exit of tube matrix, respectively. Note that the origin of the coordinate locates at the inlet of the reboiler, so $x$ increases along the yellow line from the inlet to the outlet. Since the refrigerants have different boiling temperatures, it is fair to preheat the liquid refrigerants until the inlet reach the 10 degree of sub-cooing, respectively

### 4.1 Excess temperatures

Figure 5 depicts the excess temperatures for the three refrigerants. The excess temperatures in the figure is the temperature difference between the tubes in red box in Figure 3 and the saturation temperatures of the refrigerants.

As mentioned above, for all the refrigerants, the inlet liquid temperatures are 10 K lower than their boiling temperatures, so it is fair to compare the results of $T_{excess}$ in the reboiler. Figure 5 shows that all $T_{excess}$ keep increasing from -10 K at the location close to inlet. HFE-7000 and HFE-7300 hold the same increasing trend because the properties of those two refrigerants are very close except the boiling temperatures. Water, different from the other two refrigerants, increases temperature much more slowly along the centerline of the reboiler. It is because the specific heat of water is much higher than HFE-7000 and HFE-7300. As a result, more power is needed to heat up the liquid before reaching the boiling points. In addition, an obvious slope change of $T_{excess}$ can be observed of water when $T = T_{boiling}$. It indicates the boiling starts at the moment so the temperature stops increasing, and latent heat starts to take over. When the input power is only 30 KW/m$^2$, the $T_{excess}$ of water is just above 0 after $x$ = 0.40 m, indicating boiling only occurs at the water near higher tubes. When the input power is 50 KW/m$^2$, on the other hand, near $x$ = 0.4, $T_{excess}$ has reached positive, leading to a much bigger boiling region than the low power case. The $T_{excess}$ of HFE-7000 and HFE-7300 in high power case is 20 K higher than the low power cases.

### 4.2 Vapor volume fraction

As the result of temperature increasing in the reboiler, liquid turns phase to vapor. Figure 6 (a) reveals that HFE-7000/7300 vapor starts to be observed from $x$ = 0.3 and 0.26 m when the heat flux is 30 and 50 KW/m$^2$, respectively. Then the vapor fraction of HFE-7000/7300 keeps increasing along the tube matrix. At the exit of the tube matrix, it reaches a very high value for both input powers, indicating most of the liquid has been transferred to vapor at $x$ = 0.55 m. On the other hand, as mentioned in the last section, when the input power is 30 KW/m$^2$, water starts to boil after $x$ = 0.40 m and the vapor fraction of water is just above 0.5 when it exits the tube matrix. If a higher power is applied to the reboiler (50 KW/m$^2$), water starts to boil after $x$ = 0.30 m. At the exit of the tube matrix, the high power turns more than 70% of the water to vapor near the centerline of the reboiler.

### 4.3 Phase change mass transfer rate

The mass transfer rate, which represents the mass transferred from liquid to vapor within a unit volume and unit time, is plotted in Figure 7. As discussed above, due to the similar properties, HFE-7000 and HFE-7300 still hold very similar curves in mass transfer rate, which are much higher than the one of water under the same input power. It is because water's latent heat is much greater than the other two refrigerants, leading to a very low mass transfer rate if same power is applied. The slopes mass transfer rates of HFE-7000 and HFE-7300 start to change $x$ = 0.3 and 0.26 m when the input power is 30 and 50 KW/m$^2$, respectively. The slope changes correspond to the vapor volume fraction changes of the two refrigerants where boil starts, depicting a dramatically phase change starts. The same slope change can also be observed in the water case, at about $x$ =0.4 and 0.3 m for the lower and higher power input, respectively. However, as discussed above, the value of mass transfer rate is much less than HFE-7000/HFE-7300. Comparing Figure 7 (a) and (b), it can be found that when the input power increases from 30 to 50 KW/m$^2$, the highest mass transfer rate does not increase a lot for HFE-7000/HFE-7300, because in the region ($x$ = 0.55 m), most of the liquid has been transferred to vapor as discussed above even for the low power case. The vapor fraction of water, other the other hand, shares the same trend of HFE-7000/HFE-7300, but has later start points and lower levels at the exit of the tube matrix. It is not only because the latent heat of water is much higher than HFE-7000/HFE-7300, but also because the specific heat is much greater than HFE-7000/HFE-7300.

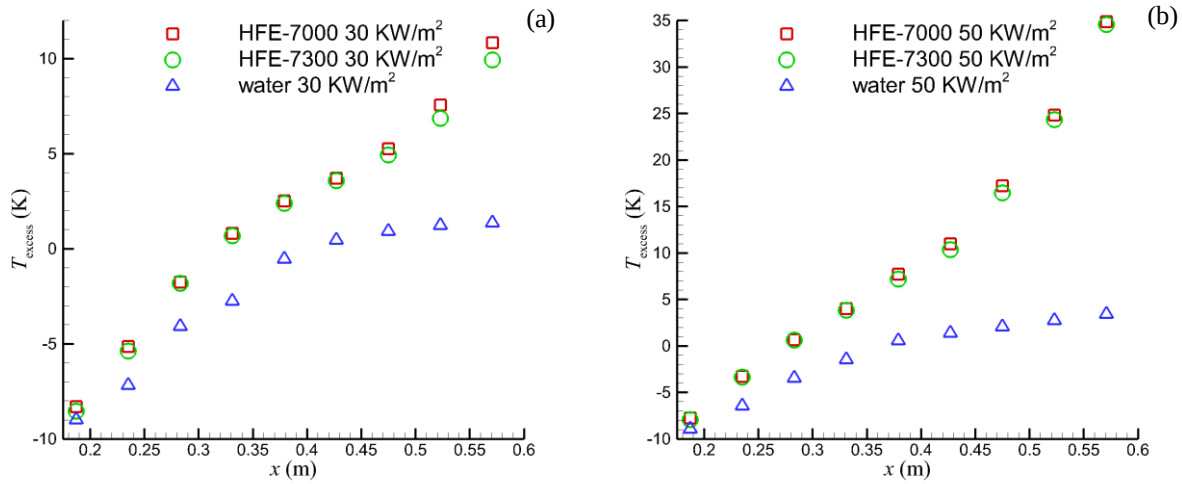


**Figure 5:** Temperature difference to the boiling temperatures for the three refrigerants along the center of the tube matrix when the tube powers are (a) 30 KW/m$^2$ and (b) 50 KW/m$^2$.

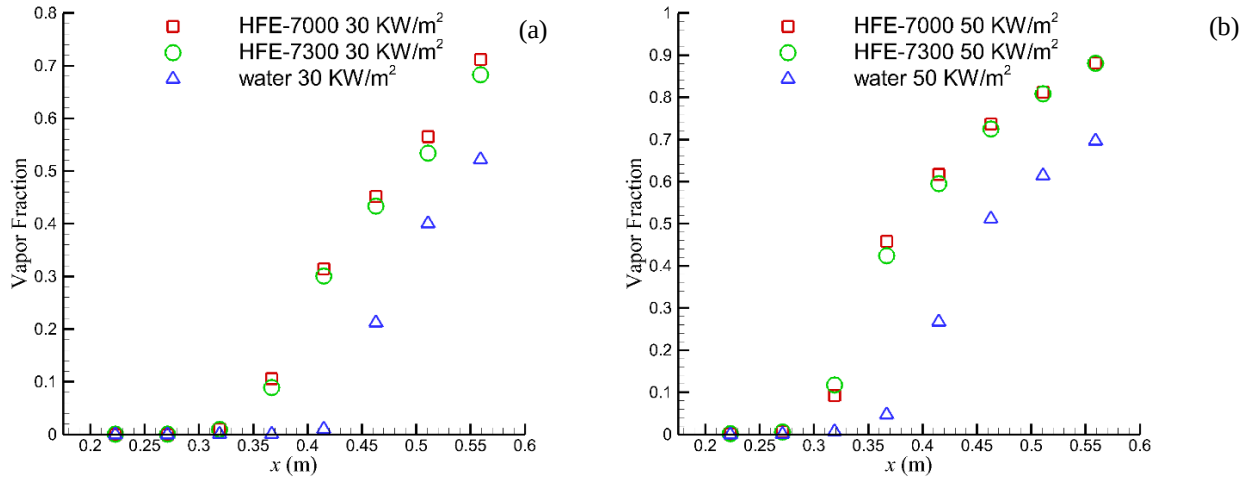


**Figure 6:** Vapor volume fraction for the three refrigerants along the center of the tube matrix when the tube powers are (a) 30 KW/m$^2$ and (b) 50 KW/m$^2$.

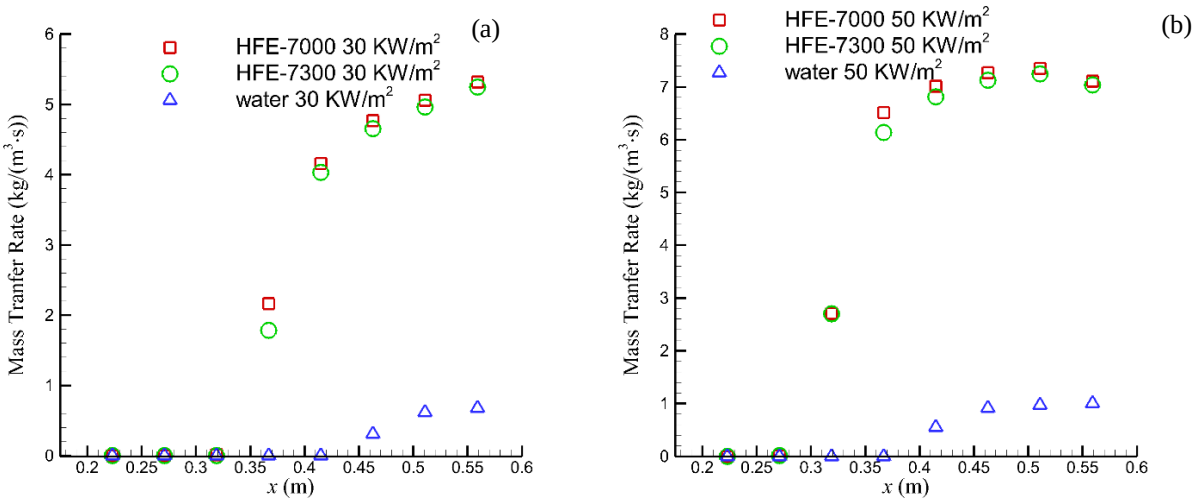


**Figure 7:** Mass transfer rate for the three refrigerants along the center of the tube matrix when the tube powers are (a) 30 KW/m$^2$ and (b) 50 KW/m$^2$.

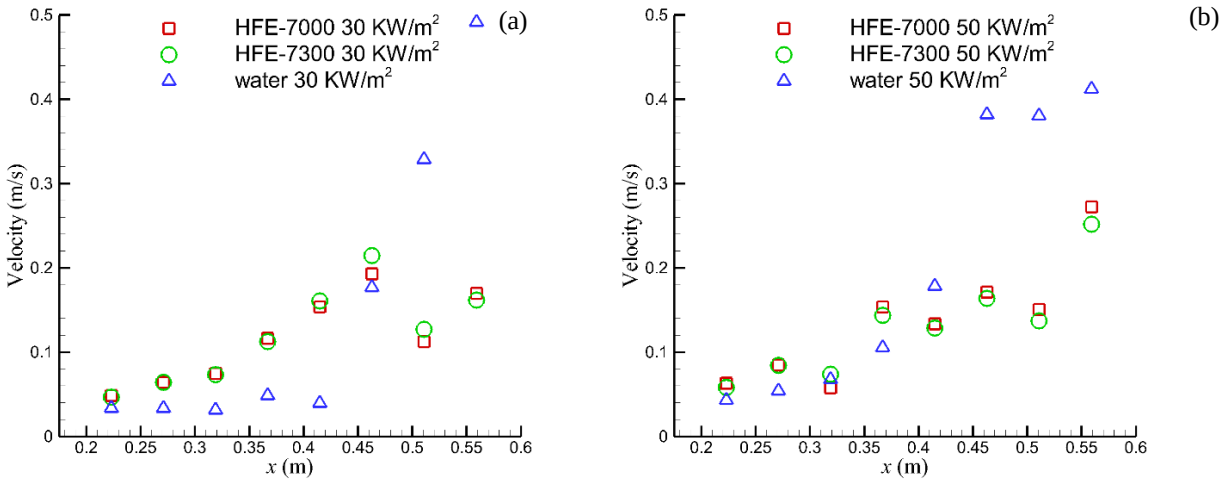


**Figure 8:** Vertical velocity of the liquid/vapor mixture for the three refrigerants along the center of the tube matrix when the tube powers are (a) 30 KW/m$^2$ and (b) 50 KW/m$^2$.

### 4.4 Vertical velocity of the liquid/vapor

Figure 8 shows the vertical velocity of the liquid/vapor for the three refrigerants along the center of the tube matrix. It shows that the velocity of water has a very rapid increasing at $x$ = 0.4 and 0.35 m when the input powers are 30 and 50 KW/m$^2$, respectively, which coincides with the vapor generation start points showing in Figure 6. The rapid speed up of water mixture is due to bubbles merging. When bubbles merge, some of the surface energy is converted to the kinetic energy leading to the velocity increasing. As a result, the buoyancy force accelerates the water mixture reaching a high velocity. However, the velocity HFE-7000/7300 does not experience the sharp increase, although the vapor start points of the two refrigerants are earlier than water. It is because the density difference between liquid/vapor of water is much greater than HFE-7000/7300, which causes a much higher buoyancy force applied to vapor than HFE-7000/7300 vapor.

## 5. CONCLUSIONS

In the present work, a two-dimensional direct CFD model has been developed to describe the flow and heat transfer in a kettle reboiler without introducing any correlations. The model has been implemented to a kettle reboiler to study the boiling process of three refrigerants: water, HFE-7000, and HFE-7300. It can be concluded that:

1. HFE-7000 and HFE-7300 have a very similar boiling behaviors except the boiling points because the properties of the two refrigerants are very close to each other.
2. The temperature of HFE-7000/HFE-7300 increases much higher than water in the reboiler with the same power input, due to the higher specific heat of water.
3. The HFE-7000/HFE-7300 generates much more vapor than water in the reboiler with the same power input, since the latent heat of HFE-7000/HFE-7300 is much lower than water.
4. The water vapor in reboiler travels much more quickly than HFE-7000/HFE-7300, due to the higher density difference between water liquid and vapor.

## REFERENCES


3M. (2009). *3M$^{TM}$ Novec$^{TM}$ 7300 Engineered Fluid*.

3M. (2014). *3M$^{TM}$ Novec$^{TM}$ 7000 Engineered Fluid*.

ANSYS. (2017). *ANSYS FLUENT 17.0 Theory Guide*.

Brisbane, T. W. C., Grant, I. D. R., & Whalley, P. B. (1980). PREDICTION METHOD FOR KETTLE REBOILER PERFORMANCE. *American Society of Mechanical Engineers (Paper), 80-HT-42*.

Burnside, B. M. (1999). 2-D kettle reboiler circulation model. *International Journal of Heat and Fluid Flow*, *20*(4), 437–445. https://doi.org/10.1016/S0142-727X(99)00024-7

Burnside, B. M., Miller, K. M., McNeil, D. A., & Bruce, T. (2001). Heat transfer coefficient distributions in an experimental kettle reboiler thin slice. *Chemical Engineering Research and Design*, *79*(4), 445–452. https://doi.org/10.1205/026387601750282373

Dowlati, R, Chan, A. M. C., & Kawaji, M. (1992). Hydrodynamics of two-phase flow across horizontal in-line and staggered rod bundles. *Journal of Fluids Engineering, Transactions of the ASME*, *114*(3), 450–456. https://doi.org/10.1115/1.2910052

Dowlati, Ramin, Kawaji, M., & Chan, A. M. C. (1990). Pitch-to-diameter effect on two-phase flow across an in-line tube bundle. *AIChE Journal*, *36*(5), 765–772. https://doi.org/10.1002/aic.690360513

Edwards, D. P., & Jensen, M. K. (1991). Two-dimensional numerical model of two-phase heat transfer and fluid flow in a kettle reboiler. *American Society of Mechanical Engineers, Heat Transfer Division, (Publication) HTD*, *159*, 9–16. https://inis.iaea.org/search/search.aspx?orig_q=RN:24019345

Hirt, C. W., & Nichols, B. D. (1981). Volume of fluid (VOF) method for the dynamics of free boundaries. *Journal of Computational Physics*, *39*(1), 201–225. https://doi.org/10.1016/0021-9991(81)90145-5

Jensen, M. K. (1988). Model for the recirculating flow in a kettle reboiler. *AIChE Symposium Series*, *84*(263), 114–119.

Lemmon;, E. W., McLinden;, M. O., & Daniel G.Friend. (2020). Thermophysical Properties of Fluid Systems. In P. J. Linstrom; & W. G. Mallard (Eds.), *NIST Chemistry WebBook, NIST Standard Reference Database Number 69* (retrieved). National Institute of Standards and Technology. https://doi.org/https://doi.org/10.18434/T4D303

McNeil, D. A., Bamardouf, K., & Burnside, B. M. (2010). A one-fluid, two-dimensional flow simulation model for a kettle reboiler. *International Journal of Heat and Mass Transfer*, *53*(5–6), 825–835. https://doi.org/10.1016/j.ijheatmasstransfer.2009.11.042

McNeil, D. A., Bamardouf, K., Burnside, B. M., & Almeshaal, M. (2010). Investigation of flow phenomena in a kettle reboiler. *International Journal of Heat and Mass Transfer*, *53*(5–6), 836–848. https://doi.org/10.1016/j.ijheatmasstransfer.2009.11.041

Noh, W., & Woodward, P. (1976). SLIC (simple line interface calculation). *Proceedings of the Fifth International Conference on Numerical Methods in Fluid Dynamics*, 330–340. https://link.springer.com/chapter/10.1007/3-540-08004-X_336

Pezo, M., Stevanovic, V. D., & Stevanovic, Z. (2006). A two-dimensional model of the kettle reboiler shell side thermal-hydraulics. *International Journal of Heat and Mass Transfer*, *49*(7–8), 1214–1224. https://doi.org/10.1016/j.ijheatmasstransfer.2005.10.004

Rahman, F. H., Gebbie, J. G., & Jensen, M. K. (1996). An interfacial friction correlation for shell-side vertical two-phase cross-flow past horizontal in-line and staggered tube bundles. *International Journal of Multiphase Flow*, *22*(4), 753–766. https://doi.org/10.1016/0301-9322(96)00015-8

Schrage, D. S., Hsu, J. -T, & Jensen, M. K. (1988). Two-phase pressure drop in vertical crossflow across a horizontal tube bundle. *AIChE Journal*, *34*(1), 107–115. https://doi.org/10.1002/aic.690340112

Stevanovic, V. D., Stosic, Z. V., Kiera, M., & Stoll, U. (2002). Horizontal steam generator thermal-hydraulics at various steady-state power levels. *International Conference on Nuclear Engineering, Proceedings, ICONE*, *3*, 767–779. https://doi.org/10.1115/ICONE10-22451

Stosic, Z. V., & Stevanovic, V. D. (2002). Advanced three-dimensional two-fluid porous media method for transient two-phase flow thermal-hydraulics in complex geometries. *Numerical Heat Transfer, Part B: Fundamentals*, *41*(3–4), 263–289. https://doi.org/10.1080/104077902753541014

## ACKNOWLEDGEMENT

This work was sponsored by the U. S. Department of Energy's Building Technologies Office under Contract No. DE-AC05-00OR22725 with UT-Battelle, LLC. We would like to acknowledge Mr. Antonio Bouza the Technology Manager for the HVAC & Appliances for his support.